Review Article: Quasi-phase-matching engineering of entangled photons

P. Xu and S. N. Zhu

Citation: AIP Advances **2**, 041401 (2012); doi: 10.1063/1.4773457
View online: http://dx.doi.org/10.1063/1.4773457
View Table of Contents: http://aipadvances.aip.org/resource/1/AAIDBI/v2/i4
Published by the American Institute of Physics.

Review Article: Quasi-phase-matching engineering of entangled photons

P. Xu[a] and S. N. Zhu[b]
National Laboratory of Solid State Microstructures and School of Physics, Nanjing University, Nanjing 210093, China

(Received 15 August 2012; accepted 17 October 2012; published online 28 December 2012)

Quasi-phase-matching (QPM) technique has been successfully applied in nonlinear optics, such as optical frequency conversion. Recently, remarkable advances have been made in the QPM generation and manipulation of photon entanglement. In this paper, we review the current progresses in the QPM engineering of entangled photons, which are finished mainly by our group. By the design of concurrent QPM processes insides a single nonlinear optical crystal, the spectrum of entangled photons can be extended or shaped on demand, also the spatial entanglement can be transformed by transverse inhomogeneity of domain modulation, resulting in new applications in path-entanglement, quantum Talbot effects, quantum imaging etc. Combined with waveguide structures and the electro-optic effect, the entangled photons can be generated, then guided and phase-controlled within a single QPM crystal chip. QPM devices can act as a key ingredient in integrated quantum information processing. [http://dx.doi.org/10.1063/1.4773457]

I. INTRODUCTION

The nonlinear crystals with modulated quadratic nonlinear coefficients $\chi^{(2)}$ are called quasi-phase-matching (QPM) materials. The concept was first referred to by Armstrong *et al.* in 1960s[1,2] and first experimentally verified by Feng and Ming *et al.*[3,4] in $LiNbO_3$ crystals with periodic ferroelectric domains by the Czochralski method in 1980s. Berger later extended the two-dimensional (2D) QPM concept from one dimension (1D) to 2D, and proposed the concept of $\chi^{(2)}$ nonlinear photonic crystal (NPC)[5] in order to contrast and compare it with a regular photonic crystal having a periodic modulation on the linear susceptibility. Since then, this artificial micro-structured material has been widely applied to the fields of nonlinear optics and laser, in particular, recently in quantum optics. The rapid development of QPM materials actually result from the breakthrough of the fabrication technique-the electrical poling technique at room temperature in 1990s.[6–8] The sign of $\chi^{(2)}$ in such a crystal is modulated by reversing the orientation of ferroelectric domain according to some sequence. The motivation for such a modulation is to achieve either a significant enhancement of nonlinear frequency conversion efficiency by QPM,[9–11] or a required wavefront of the parametric wave by nonlinear Huggens-Fresnel principle,[12–14] or for both. In history, the study for the domain modulation in a ferroelectric crystal was extended from 1D to 2D,[5,15] from periodic to quasi-periodic,[10,11,16,17] aperiodic,[18,19] even more complicated structures.[12–14] Many novel nonlinear phenomena, such as third harmonic generation,[10] nonlinear light scattering,[20,21] nonlinear Cerenkov radiation,[22] nonlinear Talbot effect[23,24] etc. were discovered from such artificial materials. Nowadays, the domain-engineered crystal has been utilized in the field of quantum optics which indicates that the study of QPM technique has entered a new regime. The bright entangled photon pairs

[a]Author to whom correspondence should be addressed. Electronic mail: pingxu520@nju.edu.cn.
[b]Electronic mail: zhusn@nju.edu.cn.

have been generated from 1D optical superlattice by spontaneously parametric down-conversion (SPDC).[25] Moreover, the generated entangled photons can been controlled with full freedom offered by designed domain structures in crystals, demonstrating two-photon focusing,[26,27] beam-splitting and other novel effects,[28–39] which can hardly be realized in a uniform nonlinear crystal. This will bring revolutionary impacts on quantum optics and quantum information science in future.

In principle, the QPM technique is endowed with several remarkable advantages in the engineering of entangled photon source. First, different from birefringence phase matching (BPM), the arbitrary polarization configuration is possible in QPM materials as long as the poling period is feasible, thereby entangled photons can be generated efficiently at any designed wavelength by using the largest nonlinearity. Secondly, spectral and spatial entanglement may be transformed by the structure design of NPC.[26–39] High-dimensional entanglement or hyper-entanglement will be generated under multiple concurrent QPM SPDC processes. In recent years, great attentions have been paid to the domain-engineered NPC for its special functionality in the integrated spectral and spatial control of entangled photons, which is inherent to the SPDC process. Finally, combined with waveguide structures and the electro-optic effect,[40] the entangled photons can be generated, then guided and phase-controlled within a single lithium niobate (LN) or lithium tantalate (LT) chip, therefore QPM materials can act as a key ingredient in integrated quantum optics. The integrated engineering of photon entanglement at the source is of fundamental importance for improving the quality of photon source and enabling the generation of new types of entangled photon source which may play a key role in the science of quantum optics and photonic quantum technologies.[41]

II. THE GENERAL TWO-PHOTON STATE FROM QPM MATERIALS

In general, the second-order nonlinearity of a two-dimensional NPC can be expressed by

$$\chi^{(2)}(x, z) = d_{eff} \sum_n F(g_n) U(x, g_n) e^{i g_n z}. \tag{1}$$

The effective nonlinearity d_{eff} is determined by the polarization configuration between the pump, the signal and idler. For LN or LT, the maximum nonlinearity d_{33} can be used when the interacted waves are all $\hat{e}$-polarized. The pump propagates along $\hat{z}$ direction. The periodic modulation of $\chi^{(2)}$ along this direction ensures the generation of entangled photon pairs by the QPM condition $k_p - k_s - k_i + g_n = 0$, in which $g_n = n\frac{2\pi}{\Lambda}$ $(n = \pm 1, \pm 2 \cdots)$ is the nth-order reciprocal vector with corresponding Fourier coefficient $F(g_n)$, and k_p, k_s, and k_i are wavevectors of the pump, the signal and the idler, respectively. $U(x, g_n)$ represents the transverse structure of the NPC which will determine the transverse amplitude and phase profile of entangled photon pair. For some simple two-dimensional structures, $U(x, g_n)$ is independent with the longitudinal structure and $\chi^{(2)}(x, z)$ follows a two-dimensional lattice with j-fold (j = 3,4,6) symmetry.

According to the interaction Hamiltonian $H_I = \varepsilon_0 \int_V d\vec{r}\, \chi^{(2)}(x, z)\{E_p^{(+)} E_s^{(-)} E_i^{(-)}\} + h.c.$, we obtain a general two-photon state based on the first-order perturbation theory,[42]

$$|\psi\rangle \propto \psi_0 \iint d\omega_s d\omega_i \iint d\vec{q}_s d\vec{q}_i \sum_n \phi_n(\omega_s, \omega_i; \vec{q}_s, \vec{q}_i) \hat{a}^{(+)}_{\omega_s, \vec{q}_s} \hat{a}^{(+)}_{\omega_i, \vec{q}_i} |0\rangle . \tag{2}$$

All the slowly varying terms and constants are absorbed into ψ_0. Here we assume more than one reciprocal vectors are participating into the QPM - SPDC processes. $\phi_n(\omega_s, \omega_i; \vec{q}_s, \vec{q}_i) = E_p(\omega_s + \omega_i) F(g_n) \int dz e^{i(k_p - k_s - k_i - g_n)z} \int d\vec{\rho} U(x, g_n) e^{i(\vec{q}_s + \vec{q}_i)\cdot\vec{\rho}}$ is the two-photon mode function which can be factorized into the spectral mode function $\phi_n(\omega_s, \omega_i) = E_p(\omega_s + \omega_i) F(g_n) \int dz e^{i(k_p - k_s - k_i - g_n)z}$ and spatial mode function $\phi_n(\vec{q}_s, \vec{q}_i) = \int d\vec{\rho} E(\vec{\rho}) U(x, g_n) e^{-i(\vec{q}_s + \vec{q}_i)\cdot\vec{\rho}}$ under the condition that the magnitude of transverse wave vectors $\vec{q}_s(\vec{q}_i)$ is much smaller than $k_s(k_i)$, i.e. satisfying $\vec{k}_j \approx k_j \hat{e}_z + \vec{q}_j$.

In the above calculations, the spectral function of pump takes the form of $E_p(\omega_p)$ and the spatial distribution follows $E_p(\vec{\rho})$. When the transverse size of pump is taken to be infinite, the spatial mode function is mainly determined by the NPC's transverse structure function $U(x, g_n)$. From Eq. (2), it is obvious that both the spectral and spatial mode functions of entangled two-photon state can be tailored by the design of NPC's structure, therefore it offers a new strategy to manipulate the entanglement in most of the degrees of freedom, like the polarization, spatial mode, frequency etc.

New types of entangled state for various applications in quantum technologies can be generated. In the paper, we will review recent progress in this field and mainly focus on the work done by our group.

III. INTEGRATED SPECTRAL ENGINEERING OF ENTANGLED PHOTONS BY QPM TECHNIQUE

The multiple QPMs device can dramatically expand the bandwidth of SPDC source.[35–39] Usually, the bandwidth of entangled photons which is mainly determined by the phase-matching condition is on the order of several THz or hundreds of GHz. To decrease or increase the bandwidth are both of great importance. Narrowband entangled photons of roughly MHz are designed to match the bandwidth of atomic ensemble-based quantum memories.[43–45] This can be achieved by an external Fabry-Perot cavity. The QPM material itself shows little advantages in narrowing the bandwidth of entangled photons. However, QPM technique is superior in engineering broadband entangled photons with relatively high efficiency, which is not possible for BPM crystals. By designing chirped QPM nonlinear crystals,[35–38] ultra broadband two-photon source can be achieved. It corresponds to the ultrashort temporal correlation toward single-cycle limit which is extraordinarily useful in clock synchronization,[46] quantum metrology,[47] and quantum optical coherence tomography.[35] An alternative and equivalent broadband source is the two-photon frequency comb.[39] One can design multiple QPM SPDC processes happening inside a single nonlinear crystal, then multiple equal spacing two-photon frequency modes can be achieved, which supplies as a natural mode-locked biphoton source since all the two-photon frequency modes come from the same original pump photon and inherit the pump's phase. The crystal can be aperiodically poled following the structure function,

$$\chi^{(2)}(z) = \chi^{(2)}\mathrm{sgn}\left\{\sum_n a_n \cos(g_n z + \phi_n)\right\} \tag{3}$$

in which g_n is the nth reciprocal vector to ensure the nth two-photon frequency mode generation. a_n and ϕ_n are adjustable parameters representing amplitude and phase for each g_n, respectively. For mode-locked two-photon source, we set reciprocal vectors to be in phase. The two-photon temporal correlation is calculated to be,[37]

$$G^{(2)}(\tau) \propto rect\left(\frac{2\tau}{DL}\right)\left\{\sin\left(\frac{N\Delta\omega\tau}{2}\right)\Big/\sin\left(\frac{\Delta\omega\tau}{2}\right)\right\}^2. \tag{4}$$

For the photon pair with a single frequency pair, the time correlation function is a rectangle function in the form of $rect(\frac{2\tau}{DL})$, whose width is determined by the group velocity dispersion $D = \frac{1}{u_s} - \frac{1}{u_i}$ and the crystal length L. u_s and u_i are the group velocities of signal and idler photons. For LT, the entangled photon pair from a 10 mm length crystal is synchronized by picoseconds precision, while for frequency-comb entangled photons from an aperiodically poled LT (APLT), the time correlation presents ultrashort pulse train in the form of $\{\sin(\frac{N\Delta\omega\tau}{2})/\sin(\frac{\Delta\omega\tau}{2})\}^2$. Figure 1[39] is a schematic second-order temporal correlation of mode-locked biphotons as well as the nondegenerate HOM interference pattern. The width of two-photon correlation peaks is determined by the mode spacing $\Delta\omega$ and the number of frequency pairs N. If the frequency comb covers as broadly as the central frequency, the width of two-photon correlation peak will approach the level of femtosecond, i.e., a single-cycle. Here, the group velocity dispersion for each frequency pair is taken to be constant, which is valid for some small dispersion materials, or the frequency comb covering not too broadly. So engineering the spectrum of entangled photons by QPM technique supplies as a unique way to shape the two-photon temporal waveform, which can be applied for exploiting new types of quantum light source, studying nonlinear optical process at single photon level and playing an important role in quantum computing.[48–50]

For a monochromatic pump, the photon pair is anti-correlated in frequency. However, this situation will be changed when extended phase matching condition is applied.[51,52] The photon pair can be correlated in frequency or noncorrelated with each other. Suppose the pump follows

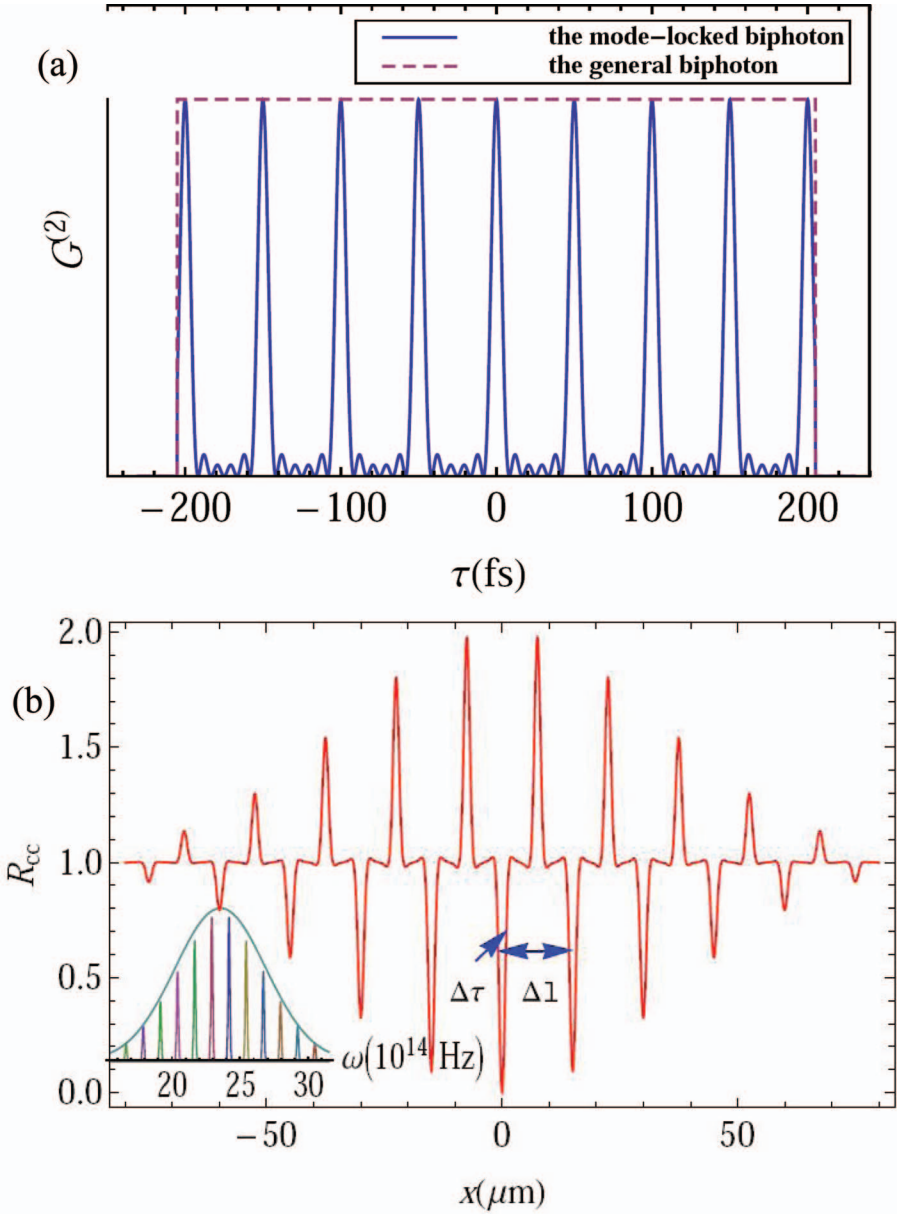

FIG. 1. (a) Comparison between time correlation of mode-locked biphotons from the APLT and that of the general biphotons from a single plain crystal. In the numerical calculation, we take $\lambda_p = 400$ nm, $\Delta\omega = 1.26 \times 10^{14}$ Hz, L = 10 mm and the number of frequency comb N = 6. The overall frequency comb covers 442 nm. The two-photon then will be mode-locked to 4.2 fs. Suppose each mode has equal spectrum width $\sigma = 6.3 \times 10^{12}$ Hz. (b) HOM interference pattern of mode-locked two-photon state when the number of frequency pairs is 6. The inset is the corresponding frequency spectrum of optical frequency comb with Gaussian Envelope. Fig. 1 is selected from literature[39] (Reproduced with permission from Y. F. Bai *et al.*, Phys. Rev. A **85**, 053807 (2012). Copyright 2012 American Physical Society).

a spectral function $E_p(\omega_p)$ and the group velocities between the pump, signal and idler satisfies a certain relationship such as $\frac{2}{u_p} = \frac{1}{u_s} + \frac{1}{u_i}$, the two-photon state will take the form of,

$$|\psi\rangle \propto \psi_0 \iint d\omega_s d\omega_i E_p(\omega_s + \omega_i) H(\omega_s - \omega_i, L) \hat{a}^{(+)}_{\omega_s} \hat{a}^{(+)}_{\omega_i} |0\rangle \tag{5}$$

in which $H(\omega_s - \omega_i, L) = \sin c\{\frac{(\omega_s - \omega_i)L}{2(u_p - u_s)}\}$ is the phase matching function ($\sin c(x) = \sin(x)/x$). Here the zero-order expansion of wavevectors has been assumed to be matched. It is straightforward that how the frequencies of photon pair are correlated depends on the comparison between the bandwidths

of pump and the phase-matching functions. For a monochromic pump, the bandwidth of pump is narrower than that of phase-matching function, thus the pair is always anticorrelated in frequency. However, frequency correlation is expected when the phase-matching condition is dominant and noncorrealation exists when the two bandwidths are comparative. Identical frequency of photon pair can improve the performance of HOM interference under a pulsed pump dispensing with any spectral filters[51,52] while the noncorrelated entangled photons will certainly benefit the applications of single photon source with better spectral purit.[53,54] However, to transform the frequency correlation requires the group velocity and phase velocity to be matched simultaneously. This may be difficult for conventional BPM crystals. But the QPM material is competent since the reciprocal vector can be designed independently with the group velocity matching condition. The two conditions never conflict in QPM materials.

IV. INTEGRATED SPATIAL ENGINEERING OF ENTANGLED PHOTONS BY QPM TECHNIQUE

Now we turn to the discussion of spatial entanglement of photon pairs from QPM materials. When studying on the spectral properties, we may assume only one spatial mode is considered, which is true for a long crystal under the plane wave pump. For a focused pump, the single spatial mode may be justified by proper spatial filters. Here, when discussing the spatial entanglement, we always assume the single frequency mode is concerned, which can be approached by narrowband spectral filters. Then we have the two-photon state in the following form

$$|\psi\rangle \propto \psi_0 \sum_{\vec{q}_s,\vec{q}_i} H_{tr}(\vec{q}_s,\vec{q}_i)\hat{a}^{(+)}_{\vec{q}_s}\hat{a}^{(+)}_{\vec{q}_i}|0\rangle . \tag{6}$$

As discussed earlier, the spatial mode function $H_{tr}(\vec{q}_s,\vec{q}_i) = \int d\vec{\rho}\, E(\vec{\rho})U(x)e^{-i(\vec{q}_s+\vec{q}_i)\cdot\vec{\rho}}$ is mainly determined by the transverse function of domain modulation and the pump profile. Several interesting two-photon effects are observed from a two-dimensional NPC including the two-photon focusing,[27] lensless ghost imaging[28] quantum Talbot effect,[29] the sub-wavelength diffraction in the far filed etc.[30]

For a simple multi-stripe PPLT (MPPLT), on one hand it works as an efficient platform for entangled photon generation under QPM condition, on the other hand its transverse periodicity engenders quantum Talbot effect directly.[29] So the quantum Talbot effect emerges dispensing with a real grating. This compact and stable self-image can be further employed for a lenless and contactless diagnosis of ferroelectric domains. The transverse structure function of modulation of MPPLT follows a grating function $U(x) = \sum_{n=-\infty}^{\infty} rect\,[(x-nd)/a]$ along x-axis with period d and stripe width a. Here $rect(x)$ is 1 for $|x| \le 1/2$ and 0 for other values. The Fourier expansion of $U(x)$ is $\sum_{n=-\infty}^{\infty} c_n e^{i2\pi nx/d}$, where $c_n = \sin(\pi na/d)/(\pi n)$ is the Fourier coefficient of the n-th harmonic. Suppose signal and idler photons are captured by detectors D_1 and D_2, respectively. When calculating the two-photon spatial correlation in the Fresnel zone, we found at certain distance from the output surface of MPPLT, coincidence counting rate between two detectors will retrieve the transverse structure of MPPLT. As long as $\frac{1}{\lambda_s z_s} + \frac{1}{\lambda_i z_i} = \frac{1}{2md^2}$, where $\lambda_{s,i}$ is the wavelength of signal or idler and m is an integer indicating the m-th Talbot plane, the two-photon coincidence counting rate

$$R_{c.c.}(x_s,z_s;x_i,z_i) = |\langle 0|\, E_1^{(+)}E_2^{(+)}\,|\psi\rangle|^2 \propto \left|\int dx_0 e^{i\pi\eta(x_0-\xi)^2}U(x_0)\right|^2$$
$$\propto \left|\sum_{n=-\infty}^{\infty} c_n e^{i2\pi n\xi/d}e^{-i\pi n^2/(d^2\eta)}\right|^2 \tag{7}$$

will turn into the grating function $U(\xi)$. A reproduction of grating function, thus the quantum Talbot effect is directly observable after the MPPLT crystal. $\xi = (\frac{x_s}{\lambda_s z_s} + \frac{x_i}{\lambda_i z_i})/(\frac{1}{\lambda_s z_s} + \frac{1}{\lambda_i z_i})$ is an associate coordinate, which means the Talbot self-image of the domain structure is magnified and the exhibited period depends on the way of detection and the wavelengths of the photon pair.

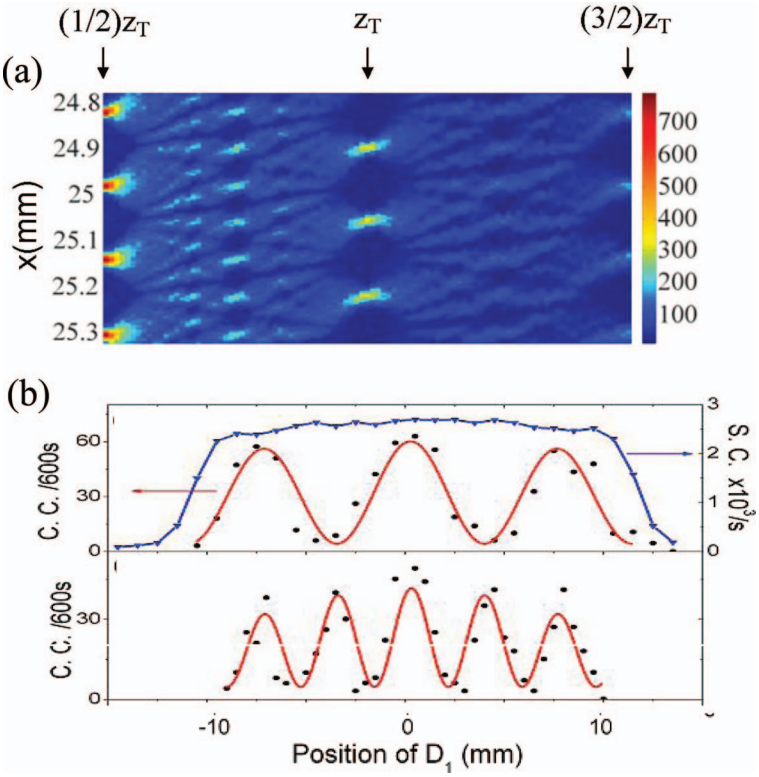

FIG. 2. The near field and far field two-photon interference pattern. The longitudinal periodicity is $\Lambda = 7.548\ \mu$m for the 1064 nm degenerate entangled photons generation. (a) Experimental two-photon Talbot carpet from $(1/2)z_T$ (48 mm) to $(3/2)z_T$ (144 mm). The transverse stripe interval is $\Lambda_{tr} = 160\ \mu$m with stripe width $b = 20\ \mu$m and stripe length $L = 10$ mm. (b) Experimental results of two-photon far-field interference in the detection plane z = 1.4 m. The transverse stripe interval is $\Lambda_{tr} = 200\ \mu$m with stripe width $b = 30\ \mu$m and stripe length $L = 6$ mm. The upper one corresponds the case that one detector is fixed and the other scans, while the lower one corresponds to the case that two detectors scan in-step. Figs. 2(a) and 2(b) are selected from literature[29] (Reprinted with permission from H. Jin *et al.*, Appl. Phys. Lett. **101**, 211115 (2012). Copyright 2012 American Institute of Physics) and literature[30] (Reproduced with permission from X. Q. Yu *et al.*, Phys. Rev. Lett. **101**, 233601 (2008). Copyright 2008 American Physical Society), respectively.

In the above calculation, $E_j^{(+)}(\vec{r}_j, t_j)$ is the electric field evaluated at the two detectors' spatial coordinate $\vec{r}_j(\vec{\rho}_j, z_j)$ $(j = s,i)$. z_s and z_i stand for the distances from the crystal to the detection planes of D_1 and D_2, respectively. The propagation of the two free-space electric fields is $E_j^{(+)}(\vec{r}_j, t_j) = \sum_{\vec{k}_j} E_j e^{-i\omega_j t_j} g(\vec{\kappa}_j, \omega_j; \vec{\rho}_j, z_j)\hat{a}_{\vec{k}_j}$, in which the Green function[42] takes the form of $g(\vec{\kappa}_j, \omega_j; \vec{\rho}_j, z_j) = \frac{-i\omega_j}{2\pi c}\frac{e^{i(\omega_j/c)z_j}}{z_j}\int d\vec{\rho}_0 e^{i\frac{\omega_j}{2cz_j}|\vec{\rho}_j - \vec{\rho}_0|^2} e^{i\vec{\kappa}_j\cdot\vec{\rho}_0}$, where $\vec{\rho}_0$ is the transverse coordinate at the output face of the crystal.

Figure 2(a)[29] is the quantum Talbot carpet observed after the MPPLT when pumped by 532 nm at 170 °C. The two detectors scanned in step for capturing a pair of 1064 nm photons. The transverse stripe interval is $\Lambda_{tr} = 160\ \mu$m with stripe width $b = 20\ \mu$m and stripe length $L = 10$ mm. The longitudinal periodicity is $\Lambda = 7.548\ \mu$m for all stripes Talbot length is calculated as $z_T = 96.2$ mm. The experimental two-photon Talbot carpet consists well with the theoretical simulations.

When exploring the two-photon far field diffraction pattern,[30] we found the coincidence counting rate takes the form of,

$$R_{c.c.}(x_s, z_s; x_i, z_i) \propto \left| H\left(\frac{\omega_s x_s}{cz_s} + \frac{\omega_i x_i}{cz_i}\right)\right|^2, \tag{8}$$

in which $H(q) = \frac{\sin(Nq\Lambda_{tr}/2)}{\sin(q\Lambda_{tr}/2)}\sin c(qb/2)$ is the far field interference-diffraction pattern for a grating, which mathematically is the Fourier transform of $U(x)$. In Eq. (8), $\xi = \frac{\omega_s x_s}{cz_s} + \frac{\omega_i x_i}{cz_i}$ is an associate

coordinate which indicates that the observed two-photon interference pattern depends on the detection scheme. When the two detectors scanned in step, the sub-wavelength diffraction will be observed[30] (Fig. 2(b)). From the near field and far field two-photon diffraction pattern, it is obvious that the domain structure can shape the spatial waveform of entangled photons. The two-photon spatial entanglement can be transformed for the purpose of certain quantum technologies.

Spatial entanglement will dramatically change when the distorted transverse structure is introduced into the NPC. By designing a transversely parabolic domain structure,[26,27] $U(x) = e^{-ig_n\alpha x^2}$, the photon pair will be self-focused after a certain distance from the crystal. In this case, the engineered crystal is equivalent to a homogeneous nonlinear crystal and a focusing lens. The spatial correlation at the focal plane is

$$R_{c.c.}(x_s, x_i)\big|_{z=f_{eff}} \propto \delta^2\left(\frac{\omega_s x_s}{cz_s} + \frac{\omega_i x_i}{cz_i}\right) \tag{9}$$

under the condition of

$$\frac{1}{\lambda_s z_s} + \frac{1}{\lambda_i z_i} = \frac{1}{\lambda_p f_{eff}}. \tag{10}$$

The pump and crystal size is assumed to be infinite. The equivalent focal length f_{eff} equals $\frac{\pi}{g_n\alpha\lambda_p}$. f_{eff} is relevant to the pump wavelength λ_p, the curvature of the parabolic NPC α and the reciprocal vector g_n for the longitudinal QPM condition. If we use a two-photon detector to capture the two-photon probability after the crystal, two-photon self-focusing will be observed as shown in Figure 3.[27] If we use two independent single photon detectors to examine the spatial correlation between the signal and idler photons, we will obtain a well-defined point to point correspondence when Eq. (10) is satisfied. This suggests an important application in lensless ghost imaging following the Gaussian thin lens equation of Eq. (10). When we put an object in one of the path, the image will be recovered in the idler path with the magnification of $-\frac{\lambda_i z_i}{\lambda_s z_s}$. When $z_s = z_i = f_{eff}$, an equal size image will be produced as shown by Fig. 4.[28]

For a multi-stripe parabolic NPC,[27,28] new characters will be brought to the two-photon lens, such as the transverse periodicity. When the pump incident at certain transverse position, a dual-focusing phenomena was observed in which the two-photon is focused onto either of two symmetric directions. In this case, the engineered crystal serves as the entangled photon source, lens and beam splitter simultaneously.[27] This multifunctional integration is free from any bulk optical elements and, therefore, may be exploited for on-chip integrated quantum optics. With these inherent linear optical elements, a lensless twin-image is observed after the same crystal.[28]

V. INTEGRATED ENGINEERING OF POLARIZATION-, PATH- AND HYPER-ENTANGLEMENT

As we know, polarization-entanglement is widely used in testing the foundations of quantum mechanics[55,56] and for developing quantum technologies.[41] A typical method to generate entangled photons relies on the type-II BPM in a nonlinear crystal[57] or two type-I crystals.[58] However, this source is less efficient since the photons pair emitted conically and only a small fraction of the cone can be collected for use. Regarding of this, beam-like entangled photons are more attractive, which can be achieved by coherently combining two SPDC sources at a polarizing beam splitter,[59–65] by manipulating polarization ququarts,[66] by overlapping two cascaded PP crystals.[67,68] However, a compact, postselection-free and bright polarization-entangled photons source is more valuable for practical applications. The cascaded[69,70] or concurrent[31,71,72] SPDC processes in a single QPM crystal can meet all the demands as shown by recent several works.

For a periodically poled LN or LT, usually only a single reciprocal vector is used to fulfill the phase-matching condition $k_p - k_s - k_i - g_1 = 0$. Degenerate or nondegenerate photon pair is generated under a certain polarization configuration. But for a dual-periodically poled crystal or other structured crystals, two concurrent QPM conditions can be satisfied simultaneously, therefore, the entangled photon pair can be generated under two possible polarization configurations, achieving $|\hat{e}_{\omega_1}\rangle|\hat{o}_{\omega_2}\rangle + |\hat{e}_{\omega_2}\rangle|\hat{o}_{\omega_1}\rangle$. Cascaded by a dichroic mirror, the nondegenerate polarization entanglement

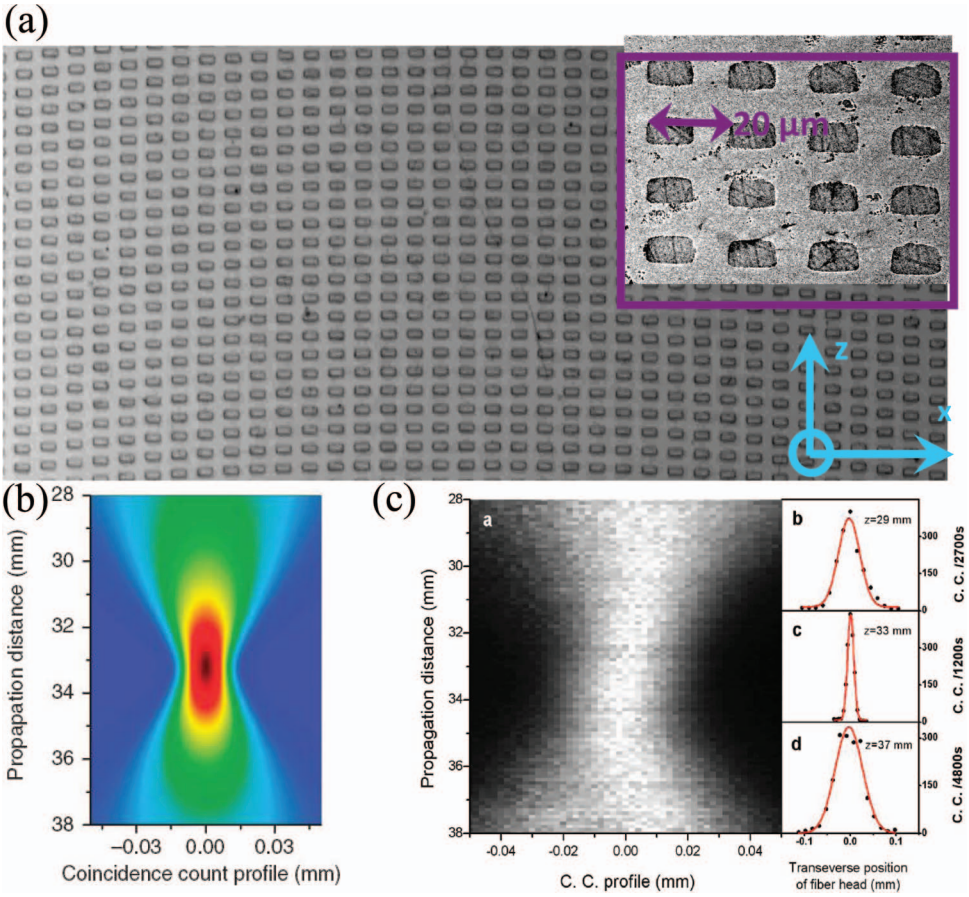

FIG. 3. (a) The micrograph of parabolic NPC. The longitudinal periodicity of NPC is $\Lambda = 13.917\ \mu$m. The third-order reciprocal vector ensures the degenerate 914 nm photon pair generation. The focal length of two-photon lens is designed to be $f_{eff} = 33.3$. The stripe interval Λ_{tr} is 20 μm, stripe width b is 10 μm and stripe length L is 6 mm. (b) The theoretical simulation of two-photon focusing dynamics under a full pump width of 0.82 mm. (c) The experimental results of two-photon focusing. The two-photon focusing spot is 28 μm, which is consistent with the theoretical value. Fig. 3(a) is selected from literature[28] (Reproduced with permission from P. Xu *et al.*, Phys. Rev. A. **86**, 013805 (2012). Copyright 2012 American Physical Society). Figs. 3(b) and 3(c) are from literature[27] (Reproduced with permission from H. Y. Leng *et al.*, Nature Commun. **2**, 429 (2011). Copyright 2011, Rights Managed by Nature Publishing Group).

is thus produced.[59,60] Furthermore, a scheme for narrowband counterpropagating polarization entangled photon pairs is proposed for realizing the natural spatial separation of degenerate photon pair.[31] So multiple QPM processes provide a new solutions for the realization of compact, beam-like and high-brightness source of polarization entangled photon pairs. In addition, by multi-stripe arrangement in a single QPM crystal, high-dimensional frequency entanglement together with polarization entanglement can be simultaneously achieved, thus a frequency- polarization hyper-entangled state may possibly be engineered,[34] which may find potential applications in quantum communication with better security and higher capacity. Furthermore, when two concurrent beam-like QPM SPDC processes exist, the cross-polarized photon pair will contribute to a bright and integrate polarization entangled state when a polarizaiton-beam-splitting is cascaded.[33] The concurrent multiple QPMs provided by the nonlinear photonic crystal open up a way to integrated quantum light sources.

The simple structured two-dimensional NPC, like a two-dimensional periodical poled LN or LT with j-fold (j = 3,4,6) symmetry is provided with the inherent advantages in the engineering of path-entanglement since multiple parametric down-conversions can happen simultaneously with a collinear or noncollinear geometry, which is crucial for path-entangled state generation.[32,33] The

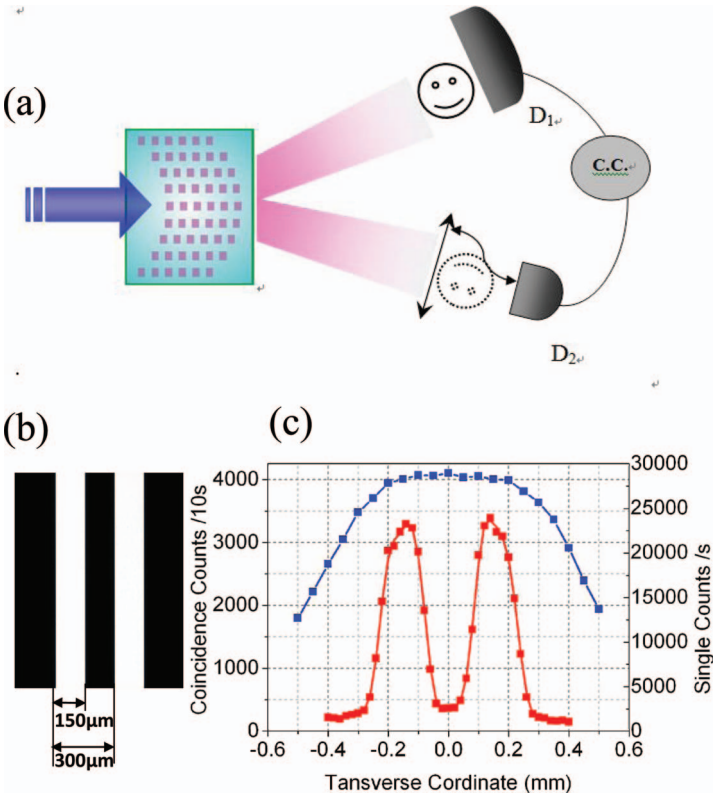

FIG. 4. (a) The schematic setup for lensless ghost imaging using entangled photons from parabolic NPC. (b) The double slit object. The slit interval is 300 μm and the slit width is 150 μm. (c) The recovered imaging by coincidence counting. Figs. 4(a) and 4(c) are selected from literature[28] (Reproduced with permission from P. Xu *et al.*, Phys. Rev. A. **86**, 013805 (2012). Copyright 2012 American Physical Society).

two-dimensional reciprocal space is expanded by

$$\chi^{(2)}(x,z) = \sum_{m,n} F(\vec{G}_{m,n}) e^{-i\vec{G}_{m,n}\cdot\vec{\rho}} \tag{11}$$

in which $\vec{G}_{m,n} = m\vec{e}_1 + n\vec{e}_2$ is reciprocal vectors. Suppose N reciprocal vectors can simultaneously participate into the SPDC processes, in general this will result in 2N spatial modes for the signal and idler photons. However, when some of the spatial modes are identically overlapped, then a two-photon multimode-entangled source will be generated. For three QPM SPDC processes happening in a rectangle NPC like Fig. 5,[32] a two-photon path-entangled state will be achieved,[32]

$$|\psi\rangle = (|2,0\rangle + |0,2\rangle + \gamma\,|1,1\rangle)/\sqrt{2+\gamma^2}. \tag{12}$$

When seeded by a two-mode coherent state, this crystal can produce two-, three-, four-, or five-photon path-entangled states in a postselection-free way.[32] In particular, up to five-photon NOON state can be generated, which enables phase supersensitive measurements at the Heisenberg limit. When a different combination of QPM geometries is adopted, a heralded single-photon multipartite entanglement can be achieved. For the multi-photon entanglement under different QPM conditions will be more interesting, especially when the path-entanglement and polarization-entanglement are simultaneously engineered.

VI. CONCLUSION

In a summary, the concurrent QPM technique enables that the flexible engineering of spatial and spectral entanglement towards the full control of photons over most degrees of freedom, enabling new types of entanglement in polarization, spatial mode, and frequency and the hyper-entanglement

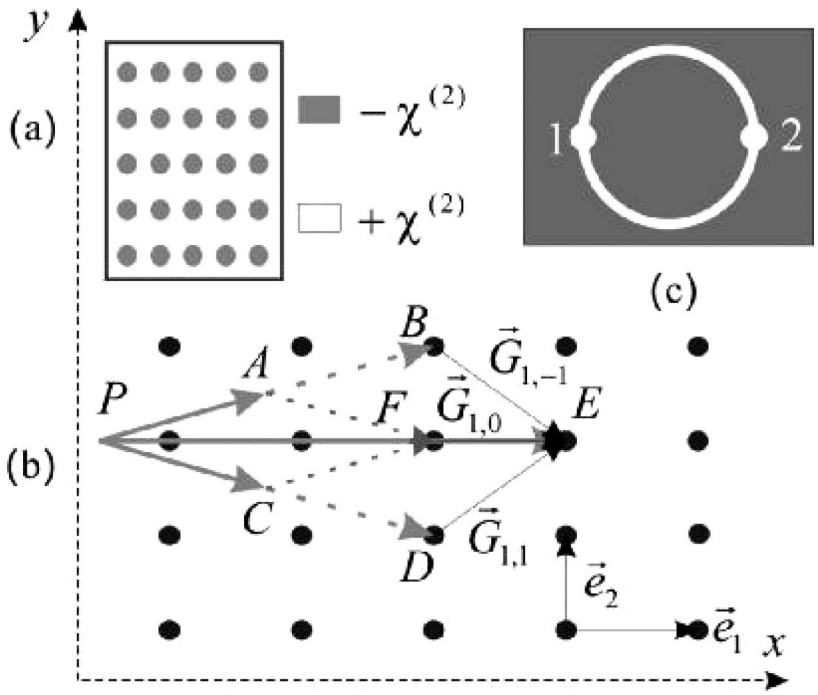

FIG. 5. (a) Schematic of a 2D NPC with a rectangular inverted domain structure. (b) the reciprocal lattice and the concurrent three QPM SPDC processes. Reciprocal lattice of the crystal. (c) Transverse pattern of the parametric light in the Fourier plane. Fig. 5 is selected from literature[32] (Reproduced with permission from Y. X. Gong *et al.*, Phys. Rev. A. **86**, 023835 (2012). Copyright 2012 American Physical Society).

over them. The new type of entangled photon source based on QPM technique may find important applications in testing quantum fundamentals, quantum communication, quantum imaging and quantum computing. It is worth noting that although the spectral and spatial properties of photon pairs in our discussion are independent, they actually affect each other.[73] For some peculiar situations, the spectral and spatial mode function can not be factorized, which deserves further consideration. Besides the natural integration function benefiting from domain engineering, LN or LT will exhibits more advantages for the integrated realization of quantum circuits after the new components like waveguides and the electro-optic effect are introduced. The electro-optics effect can offer a fast phase control of photons,[40] with a standard level of 40 GHz. The entangled source can be generated, then guided and rapidly phase-controlled within a single LN crystal. The QPM LN or LT chip will certainly be applied for integrated generation and manipulation of quantum bits soon. This will bring revolutionary impacts on quantum optics and quantum information science in future.

[1] J. Armstrong, N. Bloembergen, J. Ducuing, and P. S. Pershan, Phys. Rev. **127**, 1918 (1962).
[2] P. A. Franken and J. F. Ward, Rev. Mod. Phys. **35**, 23 (1963).
[3] N. B. Ming, *Physical Fundamentals of Crystal Growth* (Shanghai Scienti®c & Technical Publishers, Shanghai, 1982) (in Chinese).
[4] D. Feng, N. B. Ming, J. F. Hong, J. S. Zhu, Z. Yang, and Y. N. Wang, Appl. Phys. Lett. **37**, 607 (1980).
[5] V. Berger, Phys. Rev. Lett. **81**, 4136 (1998).
[6] M. Yamada, N. Nada, M. Saitoh, and K. Watanabe, Appl. Phys. Lett. **62**, 435 (1993).
[7] J. Webjörn, V. Pruneri, P. St. J. Russell, J. R. M. Barr, and D. C. Hanna, Electron. Lett. **30**, 894 (1994).
[8] S. N. Zhu, Y. Y. Zhu, Z. Y. Zhang, H. Shu, H. F. Wang, J. F. Hong, C. Z. Ge, and N. B. Ming, J. Appl. Phys. **77**, 5481 (1995).
[9] M. M. Fejer, G. A. Magel, D. H. Jundt, and R. L. Byer, IEEE J. Quantum Electron **28**, 2631 (1992).
[10] S. N. Zhu, Y. Y. Zhu, and N. B. Ming, Science **278**, 843 (1997).
[11] S. N. Zhu, Y. Y. Zhu, Y. Q. Qin, H. F. Wang, C. Z. Ge, and N. B. Ming, Phys. Rev. Lett. **78**, 2752 (1997).
[12] J. R. Kurz, A. M. Schober, D. S. Hum, A. J. Saltzman, and M. M. Fejer, IEEE J. Sel. Top. Quantum Electron. **8**, 660 (2002).
[13] Y. Q. Qin, C. Zhang, Y. Y. Zhu, X. P. Hu, and G. Zhao, Phys. Rev. Lett. **100**, 063902 (2008).
[14] T. Ellenbogen, N. Voloch-Bloch, A. Ganany-Padowicz, and A. Arie, Nature Photon. **3**, 395 (2009).
[15] N. G. R. Broderick, G. W. Ross, H. L. Offerhaus, D. J. Richardson, and D. C. Hanna, Phys. Rev. Lett. **84**, 4345 (2000).
[16] Y. Y. Zhu, and N. B. Ming, Phys. Rev. B **42**, 3676 (1990).

[17] Y. Y. Zhu and N. B. Ming, Opt. Quantum Electron. **31**, 1093 (1999).
[18] A. Norton and C. de Sterke, Opt. Express **12**, 841 (2004).
[19] J. Liao, J. L. He, H. Liu, J. Du, F. Xu, H. T. Wang, S. N. Zhu, Y. Y. Zhu, and N. B. Ming, Appl. Phys. B **78**, 265 (2004).
[20] P. Xu, S. H. Ji, S. N. Zhu, X. Q. Yu, J. Sun, H. T. Wang, J. L. He, Y. Y. Zhu, and N. B. Ming, Phys. Rev. Lett. **93**, 133904 (2004).
[21] P. Xu, S. N. Zhu, X. Q. Yu, S. H. Ji, Z. D. Gao, G. Zhao, Y. Y. Zhu, and N. B. Ming, Phys. Rev. B **72**, 064307 (2005).
[22] Y. Zhang, Z. D. Gao, Z. Qi, S. N. Zhu, and N. B. Ming, Phys. Rev. Lett. **100**, 163904 (2008).
[23] Y. Zhang, J. Wen, S. N. Zhu, and M. Xiao, Phys. Rev. Lett. **104**, 183901 (2010).
[24] Z. Chen, D. Liu, Y. Zhang, J. Wen, S. N. Zhu, and M. Xiao, Opt. Lett. **37**, 689 (2012).
[25] S. Tanzilli, H. De Riedmatten, W. Tittel, H. Zbinden, P. Baldi, M. De Micheli, D. B. Ostrowsky, and N. Gisin, Electron. Lett. **37**, 26 (2001).
[26] J. P. Torres, A. Alexandrescu, S. Carrasco, and L. Torner, Opt. Lett. **29**, 376 (2004).
[27] H. Y. Leng, X. Q. Yu, Y. X. Gong, P. Xu, Z. D. Xie, H. Jin, C. Zhang, and S. N. Zhu, Nature Commun. **2**, 429 (2011).
[28] P. Xu, H. Y. Leng, Z. H. Zhu, Y. F. Bai, H. Jin, Y. X. Gong, X. Q. Yu, Z. D. Xie, S. Y. Mu, and S. N. Zhu, Phys. Rev. A **86**, 013805 (2012).
[29] H. Jin, P. Xu, J. S. Zhao, H. Y. Leng, M. L. Zhong, and S. N. Zhu, Appl. Phys. Lett. **101**, 211115 (2012).
[30] X. Q. Yu, P. Xu, Z. D. Xie, J. F. Wang, H. Y. Leng, J. S. Zhao, S. N. Zhu, and N. B. Ming, Phys. Rev. Lett. **101**, 233601 (2008).
[31] Y. X. Gong, Z. D. Xie, P. Xu, X. Q. Yu, P. Xue, and S. N. Zhu, Phys. Rev. A **84**, 053825 (2011).
[32] Y. X. Gong, P. Xu, Y. F. Bai, J. Yang, H. Y. Leng, Z. D. Xie, and S. N. Zhu, Phys. Rev. A **86**, 023835 (2012).
[33] Y. X. Gong, P. Xu, J. Shi, L. Chen, X. Q. Yu, P. Xue, and S. N. Zhu, Opt. Lett. **37**, 4374 (2012).
[34] J. Shi, S. J. Yun, Y. F. Bai, P. Xu, and S. N. Zhu, Opt. Commun. **285**, 5549 (2012).
[35] S. Carrasco, J. P. Torres, L. Torner, A. Sergienko, B. E. A. Saleh, and M. C. Teich, Opt. Lett. **29**, 2429 (2004).
[36] S. E. Harris, Phys. Rev. Lett. **98**, 063602 (2007).
[37] M. B. Nasr, S. Carrasco, B. E. A. Saleh, A. V. Sergienko, M. C. Teich, J. P. Torres, L. Torner, D. S. Hum, and M. M. Fejer, Phys. Rev. Lett. **100**, 183601 (2008).
[38] S. Sensarn, G. Y. Yin, and S. E. Harris, Phys. Rev. Lett. **104**, 253602 (2010).
[39] Y. F. Bai, P. Xu, Z. D. Xie, Y. X. Gong, and S. N. Zhu, Phys. Rev. A **85**, 053807 (2012).
[40] D. Bonneau, M. Lobino, P. Jiang, C. M. Natarajan, M. G. Tanner, R. H. Hadfield, S. N. Dorenbos, V. Zwiller, M. G. Thompson, and J. L. O'Brien, Phys. Rev. Lett. **108**, 053601 (2012).
[41] J. L. O'Brien, A. Furusawa, and J. Vučković, Nature Photon. **3**, 687 (2009).
[42] M. H. Rubin, Phys. Rev. A **54**, 5349 (1996).
[43] Z. Y. Ou and Y. J. Lu, Phys. Rev. Lett. **83**, 2556 (1999).
[44] C. E. Kuklewicz, F. N. C. Wong, and J. H. Shapiro, Phys. Rev. Lett. **97**, 223601 (2006).
[45] X. H. Bao, Y. Qian, J. Yang, H. Zhang, Z. B. Chen, T. Yang, and J. W. Pan, Phys. Rev. Lett. **101**, 190501 (2008).
[46] A. Valencia, G. Scarcelli, and Y. Shih, Appl. Phys. Lett. **85**, 2655 (2004).
[47] V. Giovannetti, S. Lloyd, and L. Maccone, Science **306**, 1330 (2004).
[48] N. C. Menicucci, S. T. Flammia, and O. Pfister, Phys. Rev. Lett. **101**, 130501 (2008).
[49] M. Pysher, Y. Miwa, R. Shahrokhshahi, R. Bloomer, and O. Pfister, Phys. Rev. Lett. **107**, 030505 (2011).
[50] M. Pysher, A. Bahabad, P. Peng, A. Arie, and O. Pfister, Opt. Lett. **35**, 565 (2010).
[51] O. Kuzucu, M. Fiorentino, M. A. Albota, F. N. C. Wong, and F. X. K¨artner, Phys. Rev. Lett. **94**, 083601 (2005).
[52] V. Giovannetti, L. Maccone, J. H. Shapiro, and F. N. C. Wong, Phys. Rev. Lett. **88**, 183602 (2002); Phys. Rev. A **66**, 043813 (2002).
[53] Zhang *et al.*, Nature Photon. **5**, 628 (2011).
[54] A. M. Brańczyk, A. Fedrizzi, T. M. Stace, T. C. Ralph, and A. G. White, Opt. Express **19**, 55 (2011).
[55] M. Genovese, Phys. Rep. **413**, 319 (2005).
[56] Y. Shih, Rep. Prog. Phys. **66**, 1009 (2003).
[57] P. G. Kwiat, K. Mattle, H. Weinfurter, A. Zeilinger, A. V. Sergienko, and Y. Shih, Phys. Rev. Lett. **75**, 4337 (1995).
[58] P. G. Kwiat, E. Waks, A. G. White, I. Appelbaum, and P. H. Eberhard, Phys. Rev. A **60**, R773 (1999).
[59] A. Yoshizawa and H. Tsuchida, Appl. Phys. Lett. **85**, 2457 (2004).
[60] F. König, E. J. Mason, F. N. C. Wong, and M. A. Albota, Phys. Rev. A **71**, 033805 (2005).
[61] Y.-K. Jiang and A. Tomita, J. Phys. B **40**, 437 (2007).
[62] H. C. Lim, A. Yoshizawa, H. Tsuchida, and K. Kikuchi, Opt. Express **16**, 12460 (2008); **16**, 16052 (2008).
[63] S. Sauge, M. Swillo, M. Tengner, and A. Karlsson, Opt. Express **16**, 9701 (2008).
[64] M. Hentschel, H. Hübel, A. Poppe, and A. Zeilinger, Opt. Express **17**, 23153 (2009).
[65] M. Fiorentino and R. G. Beausoleil, Opt. Express **16**, 20149 (2008).
[66] E. V. Moreva, G. A. Maslennikov, S. S. Straupe, and S. P. Kulik, Phys. Rev. Lett. **97**, 023602 (2006).
[67] M. Pelton, P. Marsden, D. Ljunggren, M. Tengner, A. Karlsson, A. Fragemann, C. Canalias, and F. Laurell, Opt. Express **12**, 3573 (2004).
[68] D. Ljunggren, M. Tengner, P. Marsden, and M. Pelton, Phys. Rev. A **73**, 032326 (2006).
[69] T. Suhara, G. Nakaya, J. Kawashima, and M. Fujimura, IEEE Photon. Technol. Lett. **21**, 1096 (2009).
[70] W. Ueno, F. Kaneda, H. Suzuki, S. Nagano, A. Syouji, R. Shimizu, K. Suizu, and K. Edamatsu, Opt. Express **20**, 5508 (2012).
[71] K. Thyagarajan, J. Lugani, S. Ghosh, K. Sinha, A. Martin, D. B. Ostrowsky, O. Alibart, and S. Tanzilli, Phys. Rev. A **80**, 052321 (2009).
[72] Z. H. Levine, J. Fan, J. Chen, and A. L. Migdall, Opt. Express **19**, 6724 (2011)
[73] C. I. Osorio, A. Valencia, and J. P. Torres, New J. Phys. **10**, 113012 (2008).